UDC 621.396.962

TWO-FRAGMENT NON-LINEAR-FREQUENCY MODULATED SIGNALS WITH ROOTS OF QUADRATIC AND LINEAR LAWS FREQUENCY CHANGES

Kostyria O. O. – Dr. Sc., Senior Research, Leading Research Scientist, Ivan Kozhedub Kharkiv National Air Force University, Kharkiv, Ukraine.

Hryzo A. A. – PhD, Associate Professor, Head of the Research Laboratory, Ivan Kozhedub Kharkiv National Air Force University, Kharkiv, Ukraine.

Khudov H. V. – Dr. Sc., Professor, Head of Department, Ivan Kozhedub Kharkiv National Air Force University, Kharkiv, Ukraine.

Dodukh O. M. – PhD, Leading Research Scientist, Ivan Kozhedub Kharkiv National Air Force University, Kharkiv, Ukraine.

Lisohorskyi B. A. – PhD, Senior Researcher, Ivan Kozhedub National Air Force University, Kharkiv, Ukraine.

ABSTRACT

Context. The rapid development of the technology of digital synthesis and processing of radar signals, which has been observed in recent decades, has practically removed restrictions on the possibility of implementing arbitrary laws of frequency modulation of radio oscillations. Along with the traditional use of linearly-frequency-modulated signals, modern radar means use probing signals with non-linear frequency modulation, which provide a lower level of maximum side lobes and a higher rate of their descent. These factors, in turn, contribute to improving the detection characteristics of targets under conditions of passive interference, as well as increasing the probability of detecting small targets against the background of targets with larger effective scattering surfaces. In this regard, a large number of studies are conducted in the direction of further improvement of existing and synthesis of radar signals with new laws of frequency modulation. The use of multifragment nonlinear-frequency-modulated signals, which include fragments with both linear and nonlinear modulation, provides an increase in the number of possible versions of the laws of frequency modulation and synthesis of signals with predicted characteristics. Synthesis of new multifragment signals with a reduced level of side lobes of autocorrelation functions and a higher rate of their descent is an important scientific and technical task, the solution of which is devoted to this article.

Objective. The purpose of the work is to develop mathematical models of the current and shifted time of two-fragment nonlinear-frequency modulated signals for the case when the first fragment has a root-quadratic, and the second linear frequency modulation and determine the feasibility of using such a signal in radar applications.

Method. The article theoretically confirms that for the mathematical model of the current time, when moving from the first fragment to the second at the junction of fragments, jumps of instantaneous frequency and phase (or only phases for the mathematical model of shifted time) occur, which can significantly distort the resulting signal. Determination of value of frequency-phase jumps for their further elimination is performed by finding difference between value of initial phase of second fragment and final value of phase of first fragment. A distinctive feature of the developed mathematical models is the use of the first fragment of the signal with root-quadratic, and the second – linear frequency modulation.

Results. Comparison of the signal, the first fragment of which has root-square frequency modulation, and the signal with two linearly-frequency-modulated fragments, provided that the total duration and frequency deviation are equal, shows that for the new synthesized signal the maximum level of side lobes decreased by 1.5 dB, and their rate of decay increased by 6.5 dB/dec.

Conclusions. A new two-fragment signal was synthesized, the first fragment of which has root-quadratic, and the second – linear frequency modulation. Mathematical models of the current time and with a time shift for calculating the values of the instantaneous phase of such a signal have been developed. A distinctive feature of these models is the presence of components to compensate for frequency-phase distortions, taking into account the modulation law of the frequency of the first fragment. The resulting oscillograms, spectra and autocorrelation functions of the synthesized two-fragment signals do not contradict the known theoretical position, which indicates the reliability and adequacy of the proposed mathematical models.

KEYWORDS: mathematical model; non-linear frequency modulation; maximum level of side lobes.

ABBREVIATIONS

ACF is an autocorrelation function;
SL is a side lobe;
ML is a main lobe;
PWM is a pulse-width modulation;
WP is a weight processing;
RQFM is a roots of quadratic frequency modulation;
LFM is a linear frequency modulation;
MM is a mathematical model;
MPSLL is a maximum peak side lobe level;
NLFM is a non-linear frequency modulation;
PSLL is a peak side lobe level;
REQ is a radio electronic equipment
RP is a radio pulse;
FM is a linear frequency modulation;
FMR is a frequency modulation rate;
DDS is a digital discrete synthesis;
DSP is a digital signal processor;
FPGA is a field-programmable gate array;
SDR is a software-defined radio;
PLL is a phase-locked loop.

DOI 10.15588/1607-3274-2024-1-2

NOMENCLATURE

B_S is a time-bandwidth product;

Δf_S is a frequency deviation of the signal, Hz;

Δf_n is a frequency deviation of the n^{th} signal fragment NLFM, Hz;

T_S is a weight of the signal, s;

n=1, 2 is a serial number signal fragment NLFM;

f_0 is a initial signal frequency, Hz;

t is a current time, s;

T_n is a duration of the n^{th} signal fragment NLFM, s;

T_{12} is a sums of duration of the first and second fragments, s;

$\varphi_n(t)$ is a instantaneous phase n-го signal fragment NLFM, rad;

β_n is a FMR n^{th} signal fragment NLFM, Hz/s;

$\Delta\beta_{21}$ is a difference FMR 2nd and 1th fragments, Hz/s;

β_{1N} is a average FMR 1th fragment, Hz/s;

β_{1E} is a ultimate FMR 1th fragment, Hz/s;

$\delta\varphi_{12}$ is a component to compensate for phase jump at fragment junction, rad.

.

INTRODUCTION

The widespread use of digital synthesis and radar signal processing due to the introduction of new capabilities of DDS, DSP, FPGA, SDR technologies [1–10] provides the use of signals with various types of PWM [11–16]. Signals with PWM frequency (phase) are called complex signals, among them the most widely used are signals with LFM. Such signals ensure preservation of required distinguishing ability from range in case of increase of radar probing signal duration to increase its energy potential [11–13, 15, 17–22]. Scientific research is actively carried out to improve the technical characteristics of REQ by using complex signals with different types of PWM from LFM, one of the directions is to minimize the value of MPSLL ACF radar signals.

As a rule, this is achieved by selecting the type of modulation of the probe signal [11–24] or by WP of the reflected radio frequency oscillation in the radar receiver [25, 26]. It is also possible to jointly apply the above methods [27–29], which can potentially provide a better result. The effectiveness of the use of WP depends significantly on such a parameter as the rate of decrease in the SL of ACF signals. Therefore, when selecting a probe signal, in addition to the MPSLL, attention should also be paid to the value of the SL descent rate, which should be as achievable as possible.

The choice of the PWM type of the probe signal can be based on the analysis of its spectral characteristics – a sign of a decrease in the ACF MPSLL is the rounding of the signal spectrum, that is, the approximation of its shape to the bell-shaped one. This effect can be achieved by using nonlinear frequency modulation, namely, by increasing the FM, which is a derivative of the instantaneous frequency $\beta(t) = df(t)/dt$. In this case, the FM can have both a constant (linear frequency change) and a variable value (non-linear FM). Such signals are related to NLFM signals, they can be formed by sequentially joining fragments in time with linear and nonlinear FM. There are MM two- and three-fragment NLFM signals [30–34]. Single-fragment signals with polynomial, tangential, S-shaped and other types of FM are also known [35–39]. NLFM signals also include phase-manipulated signals [41].

This article is devoted to the consideration of the features of the formation of multi-fragment, namely two-fragment NLFM signals.

There is no doubt that three-fragment NLFM signals provide lower MPSLL compared to two-fragment signals, and therefore their use is more expedient. However, two-fragment signals should not be excluded from consideration, since they are significantly easier to implement, richly illustrative and allow more efficient testing of new theoretical hypotheses and putting into practice the results obtained. Such signals should be used at the initial stage of research to debug MM and develop software products for their practical reproduction.

The research is based on the hypothesis that it is possible to synthesize an NLFM signal with a lower MPSLL and a higher rate of decline of the SL if one of the fragments in the low frequency region has a more rounded shape.

The article considers the case when the first fragment of the NLFM signal has a root-quadratic, and the second – linear FM.

The object of study is the process of forming and processing two-fragment NLFM signals.

The subject of study are mathematical models of NLFM signals, which consist of two fragments of the RQFM-LFM type.

The purpose of the work is to develop the MM of the current and shifted time of the RQFM-LFM signal and determine the feasibility of using such a signal in radar applications.

1 PROBLEM STATEMENT

The authors [33], along with NLFM signals, which consist of LFM fragments, consider signals, one of the fragments of which has a nonlinear law of frequency change, for example, exponential. They are also considered as independent tangential, polynomial, S-shaped and other laws of frequency modulation [14, 35–39], which provide two-sided or one-sided rounding of the signal spectrum.

A distinctive feature of the signal with RQFM in comparison with the classical LFM signal is the rounding of the spectrum in the low frequency region, which makes it attractive to use it as one of the fragments for the synthesis of multi-fragment NLFM signals. It is to be expected that the NLFM signals, when included in their composition of the RQFM fragment, will have better

DOI 10.15588/1607-3274-2024-1-2

characteristics with MPSLL compared to signals consisting only of LFM fragments.

To determine the features of the synthesis of NLFM signals using RQFM fragments, it is proposed to first consider the option of a two-fragment RQFM-LFM signal with the development of the current and shifted time MM.

The authors of the article propose to consider two-fragment NLFM signals, the first fragment of which has RQFM, that is, its instantaneous frequency changes in accordance with the expression:

$$f_1(t) = f_0 + \beta_{1N}\sqrt{T_1 t}\,, \qquad (1)$$

where $\beta_{1N} = \dfrac{\Delta f_1}{T_1}$ – average FMR 1th fragment RQFM NLFM signal.

As the initial, let's take the MM of the current time of the NLFM signal with frequency-phase distortion compensation, which consists of two LFM fragments [40]:

$$\varphi(t) = \begin{cases} 2\pi\left[f_0 t + \dfrac{\beta_1 t^2}{2}\right], 0 \le t \le T_1; \\ 2\pi\left[(f_0 - \Delta\beta_{21} T_1)t + \dfrac{\beta_2 t^2}{2}\right] + \delta\varphi_{12}, T_1 \le t \le T_{12}; \end{cases} \qquad (2)$$

where $\delta\varphi_{12} = \pi T_1^2 \beta_{21}$; $\beta_n = \Delta f_n / T_n$; $\Delta\beta_{21} = \beta_2 - \beta_1$; $T_{12} = T_1 + T_2$.

The current instantaneous phase component, which compensates for frequency jumps during the transition from the first fragment to the second, is calculated as $\Delta\beta_{21} T t$.

As the initial MM shifted time, we also use the NLFM signal with two LFM fragments [41] of the form:

$$\varphi_n(t) = \begin{cases} 2\pi\left[f_0 t + \dfrac{\beta_1 t^2}{2}\right], 0 \le t \le T_1; \\ 2\pi\left[(f_0 + \Delta f_1)(t - T_1) + \beta_2\left(\dfrac{t^2}{2} - T_1 t\right)\right] - \delta\varphi_{12}, \\ T_1 \le t \le T_{12}. \end{cases} \qquad (3)$$

where $\delta\varphi_{12} = -\pi T_1^2(\beta_2 + \beta_1)$.

It is expected that due to the instantaneous change in FMR at the joints of RQFM and LFM fragments, instantaneous frequency and phase jumps (or only phases for MM shifted time) will occur, as is justified in [40, 41], but the expressions for calculating the magnitude of these jumps will be different, and therefore the resulting MM will be new, which is the result research.

The effectiveness of the use of new MMs is evaluated by achievable MPSLL, the rate of reduction of SL and the width of ML ACF signals, which is measured at 0.707 of the maximum value, compared to the previously obtained in the works [14, 27–41]. Also, when comparing the results obtained, the value of the signal base should be taken into account $B_S = \Delta f_S T_S$, that is, the product of the deviation of the signal frequency by its duration, since with a decrease in B_S, the MPSLL ACF value usually increases.

2 REVIEW OF THE LITERATURE

New opportunities for digital synthesis and digital processing of radar signals, which are provided by DDS, DSP, FPGA, SDR technologies, allow to radically revise approaches to the development of a new and improvement of the existing REQ. The stimulator of this process is DDS [1, 2], which provides the development of increasingly high-frequency radio bands. The emergence of such a tool as DSP [3, 4] at one time made a significant improvement in the efficiency of DSP systems in relation to the range of operating frequencies and their band. In the future, the FPGA [5–9] combines DDS with PLL, provides DSP functions, which allows you to quickly change the operating modes of radar equipment by changing the operating frequency, type of probe signal and operating frequency band. SDR technology [10] is now more of a tool for scientific researchers and REQ developers, as due to versatility it can have excessive hardware redundancy.

The above indicates that there is a practical possibility of introducing new types of probing signals with different types of PWM into REQ.

Theoretically, the feasibility of using probing LFM and RQFM signals [11–13, 15, 17–22], which historically were the first among complex signals, has been proved in practice. The authors of these publications define as complex such signals, the base of which, that is, the product of the duration of RP by the width of its frequency band, is more than one. In addition to LFM and RQFM, signals with non-linear PWM frequencies – NLFM signals [11–24, 27–41] are also complex.

The nonlinear PWM frequency allows increasing FRM at the edges of the RP, as a result of which the signal spectrum is rounded, which is equivalent to the WP signal in the time domain [25, 26], but the bypass RP remains rectangular and the energy loss in the radio transmitter does not increase.

Varieties of NLFM signals are widely considered by the authors [14, 27–41], these works are devoted to the problem of improving the characteristics of REQ by reducing MPSLL, which is achieved due to the WP signal in the radio receiver [25, 26], rounding the signal spectrum [14, 30–41] or the simultaneous use of these methods [27–29].

Reduction of MPSLL can be achieved by synthesizing a new type of signal, as described in [33]. The authors proposed a two-fragment NLFM signal, the first fragment of which has an exponential FM.

It is appropriate to clarify the feasibility of using fragments with other non-linear types of FM, which can

DOI 10.15588/1607-3274-2024-1-2

also provide rounding of the signal spectrum and reduce MPSLL.

New opportunities for digital synthesis and digital processing of radar signals, which are provided by DDS, DSP, FPGA, SDR technologies, allow to radically revise approaches to the development of a new and improvement of the existing REQ. The stimulator of this process is DDS [1, 2], which provides the development of increasingly high-frequency radio bands. The emergence of such a tool as DSP [3, 4] at one time made a significant improvement in the efficiency of DSP systems in relation to the range of operating frequencies and their band. In the future, the FPGA [5–9] combines DDS with PLL, provides DSP functions, which allows you to quickly change the operating modes of radar equipment by changing the operating frequency, type of probe signal and operating frequency band. SDR technology [10] is now more of a tool for scientific researchers and REQ developers, as due to versatility it can have excessive hardware redundancy.

The above indicates that there is a practical possibility of introducing new types of probing signals with different types of PWM into REQ.

Theoretically, the feasibility of using probing LFM and RQFM signals [11–13, 15, 17–22], which historically were the first among complex signals, has been proved in practice. The authors of these publications define as complex such signals, the base of which, that is, the product of the duration of RP by the width of its frequency band, is more than one. In addition to LFM and RQFM, signals with non-linear PWM frequencies – NLFM signals [11–24, 27–41] are also complex.

The nonlinear PWM frequency allows increasing FRM at the edges of the RP, as a result of which the signal spectrum is rounded, which is equivalent to the WP signal in the time domain [25, 26], but the bypass RP remains rectangular and the energy loss in the radio transmitter does not increase.

Varieties of NLFM signals are widely considered by the authors [14, 27–41], these works are devoted to the problem of improving the characteristics of REQ by reducing MPSLL, which is achieved due to the WP signal in the radio receiver [25, 26], rounding the signal spectrum [14, 30–41] or the simultaneous use of these methods [27–29].

Reduction of MPSLL can be achieved by synthesizing a new type of signal, as described in [33]. The authors proposed a two-fragment NLFM signal, the first fragment of which has an exponential FM.

It is appropriate to clarify the feasibility of using fragments with other non-linear types of FM, which can also provide rounding of the signal spectrum and reduce MPSLL.

3 MATERIALS AND METHODS

Using the methods [40] and (1), we determine the final phase of the first fragment and the initial phase of the second fragment of the RQFM-LFM signal for the time $t=T_1$. It should be noted that the FMR of a fragment with RQFM is a time variable, its instantaneous value is:

$$\beta_1(t)=\frac{\beta_{1N}}{2}\sqrt{\frac{T_1}{t}}$$

and at time $t=T_1$, the final FMR value is:

$$\beta_{1E}=\beta_1(T_1)=\frac{\beta_{1N}}{2}. \quad (4)$$

We have expressions for the final phase of the first and the initial phase of the second fragment:

$$\varphi_{E1}=2\pi\left(f_0T_1+\frac{2}{3}\beta_{1E}T_1^2\right); \quad (5)$$

$$\varphi_{S2}=2\pi\left(f_0T_1+\frac{1}{2}\beta_2T_1^2\right) \quad (6)$$

and taking into account (4)–(6) the phase jump at the junction of the fragments is equal to:

$$\delta\varphi_{12}=2\pi T_1^2\left(\frac{\beta_2}{2}-\frac{\beta_{1N}}{3}\right). \quad (7)$$

Thus, based on (1), (2) and (7), the MM for calculating the instantaneous phase of the two-fragment NLFM signal in the current time, if the frequency of the first fragment changes according to the root-square law, has the form:

$$\varphi(t)=\begin{cases}2\pi\left[f_0t+\dfrac{2\beta_{1N}\sqrt{t^3T_1}}{3}\right], 0\le t\le T_1;\\ 2\pi\left[\left(f_0-\Delta\beta_{21}T_1\right)t+\dfrac{\beta_2t^2}{2}\right]-\delta\varphi_{12},\ T_1\le t\le T_{12}\end{cases}. \quad (8)$$

An MM of the current time of the two-fragment NLFM signal (8) is obtained, which provides determining a frequency jump at the junction of fragments in the case when the first fragment is a signal from RQFM, which, in turn, allows compensating for the corresponding phase jump and taking into account the change in instantaneous frequency when switching to the second fragment.

These results can be applied to the development of an MM shifted time for a similar signal in which the frequency jump at the junction of fragments is compensated automatically.

Using (1), (3), (4) and the results of the studies [41], the phase jump at the fragment junction for MM shifted time is defined as:

$$\delta\varphi_{12}=-\pi T_1^2\left(\beta_2+\frac{4\beta_{1N}}{3}\right). \quad (9)$$

DOI 10.15588/1607-3274-2024-1-2

Using (1), (3) and (9), we record the MM of the shifted time to calculate the instantaneous phase of the two-fragment NLFM signal, the first fragment of which is the signal from RQFM:

$$\varphi(t) = \begin{cases} 2\pi\left[f_0 t + \frac{2\beta_{1N}\sqrt{t^3 T_1}}{3}\right], 0 \le t \le T_1; \\ 2\pi\left[(f_0 + \Delta f_1)(t - T_1) + \frac{\beta_2(t^2 - T_1 t)}{2}\right] - \delta\varphi_{12},\ T_1 \le t \le T_{12} \end{cases} \quad (10)$$

Model (10) differs from (8) in the form of time representation and is fully adequate to it. That is, (8) and (10) allow you to get the same final result in different mathematical ways, which is evidence of their fairness and reliability.

4 EXPERIMENTS

The operability of the two-segment NLFM signals developed by MM, in which the first fragment has RQFM, was checked using the MATLAB application package.

To determine the advantages and disadvantages of the new synthesized RQFM-LFM signal, three more complex signals were simulated: single-fragment (LFM, RQFM) and two-fragment (LFM-LFM) with equivalently identical frequency-time parameters. That is, the total duration and frequency deviation of two-fragment signals is equal to the duration and frequency deviation of single-fragment signals that were taken for research. The following signal characteristics were measured and compared:

– MPSLL value;

– SL descent rate;

– ML ACF signal width at the level of 0.707 of the maximum value.

For a more detailed analysis of RQFM-LFM signals, a group of five signals was studied, for one of which graphic material was provided. Also, for comparison, a graphic material for single-fragment LFM and RQLF signals was obtained, the frequency-time parameters of which coincide with the parameters of one of the RQLF-LFM signals (No. 3, Table 2).

5 RESULTS

The results of studies of single-fragment LFM, RQFM and two-fragment LFM-LFM, RQFM-LFM signals are summarized in Table 1.

Comparison of results for LFM and RQFM signals shows that the RQFM signal has a larger ML ACF width, this is evidence of a decrease in the effective signal spectrum width, which is perfectly logical, since the LFM spectrum of Fig. 1a compared to the RQFM spectrum of Fig. 2b has a more rectangular shape, that is, in the same frequency band, the power spectral density of the RQFM signal is less than that of the LFM signal.

Table 1 – Results of experimental studies of NLFM signals of different types with equivalent frequency-time parameters

Type of signal	T_1, μs	T_2, μs	Δf_1, kHz	Δf_2, kHz	MPSLL, dB	Decline of SL, dB/s	ML ACF, μs
LFM	120	–	600	–	–13.43	19.65	0.75
RQFM	120	–	600	–	–13.47	19.55	0.92
LFM-LFM	20	100	200	400	–17.31	17.42	0.83
RQFM-LFM	40	80	400	200	–19.0	24.0	1.03

The MPSLL values and the SL decay rates of these signals are virtually indistinguishable.

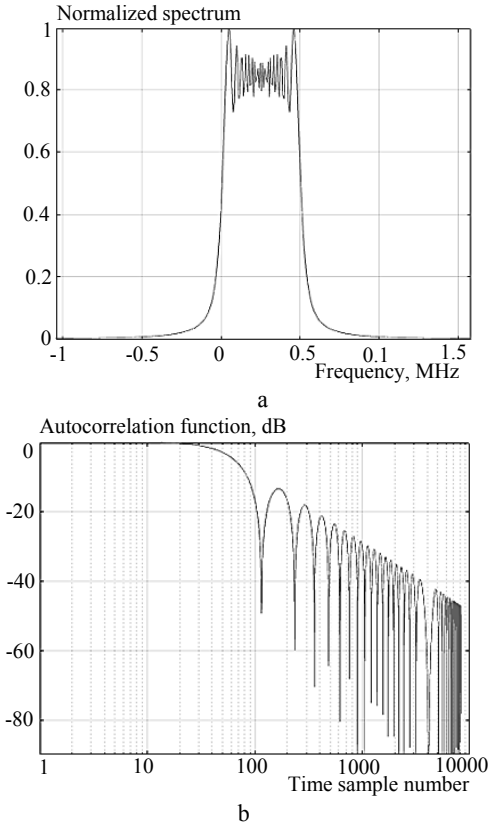

Figure 1 – Spectrum (a), ACF (b) LFM signal

It should be noted that the amplitude of the pulsations of the SL ACF LFM signal (spurious oscillations at the output of the matched filter) exceeds 20 dB (Fig. 1b), for the RQFM signal this value averages 5 dB (Fig. 2c), and therefore the use of WP for such signals should give the best effect.

Table 2 shows the values of frequency-time parameters of the studied two-fragment RQFM-LFM signals calculated in accordance with MM (8). The use of MM (10) provides identical results.

DOI 10.15588/1607-3274-2024-1-2

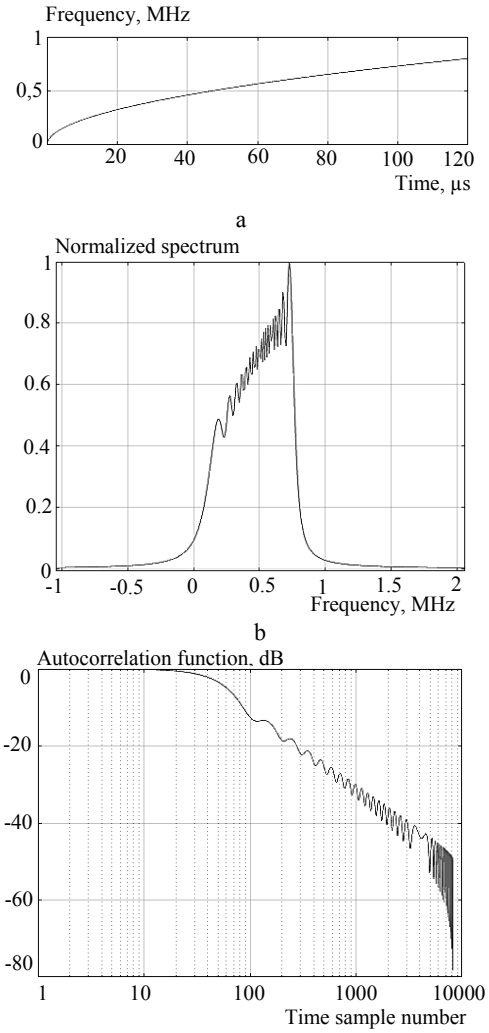

Figure 2 – Frequency change plot (a), spectrum (b), ACF (c) signal with RQFM

Table 2 – Results of experimental studies of two-fragment RQFM-LFM signals

No	T_1, μs	T_2, μs	Δf_1, kHz	Δf_2, kHz	MPSLL, dB	Decline of SL, dB/s
1.	20	40	500	300	–20.76	21.5
2.	40	80	500	100	–20.0	26.5
3.	40	80	500	300	–19.71	22.3
4.	80	160	500	300	–19.38	22.6
5.	80	160	600	400	–20.16	20.0

A comparative analysis of the results of Table 1 and Table 2 indicates that, provided the frequency-time parameters of signals such as RQFM-LFM and LFM-LFM are equal, the MPSLL decrease for the new signal is approximately from 1.5 dB to almost 2.7 dB, and the SL decrease rate increase in this case, from 6.6 dB/dec. up to 9.1 dB/deck.

The result of comparing the graphic material for RQFM (Fig. 2) and RQFM-LFM (Fig. 3) signals is interesting. Graphs of the instantaneous frequency change over time in Fig. 2a and Fig. 3a have insignificant differences at the mark of 40 μs – Fig. 3a shows a slight decrease in the characteristic. In this case, the signal spectra of Fig. 2b and Fig. 3b differ significantly. Figure 3b clearly shows both spectral components of the signal, the transition between them without gaps and differences. That is, there are no frequency and phase jumps at the junction of the fragments.

Based on the results of comparative analysis of ACF signals, the following should be noted. As a result of the combination of two types of FM, the first SL RQFM signal (see. Fig. 2c) on the ACF graph, the RQFM-LFM signal merged with ML (Fig. 3c), as a result of which the width of ML at the minimum level increased, the dip between the first SL and the second SL increased, as a result of which the level of the second SL from –18 dB decreased to –22 dB and the third petal became the maximum at –20 dB. The amplitude of pulsations SL in Fig. 3v compared to Fig. 2b increased by 2–3 dB, but it is significantly less than for the single-fragment LFM signal Fig. 1b. These changes with other digital values are observed in the ACF graphs of RQFM-LFM signals with identical frequency-time parameters, which are included in Table 2.

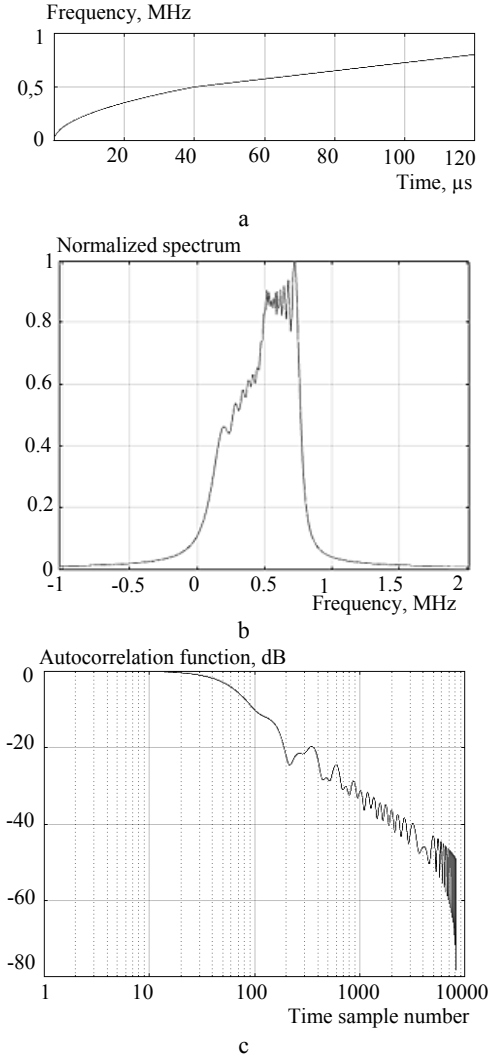

Figure 3 – Frequency change plot (a), spectrum (b), ACF (c) signal from RQFM-LFM

DOI 10.15588/1607-3274-2024-1-2

To demonstrate the potentially achievable characteristics, Fig. 4 shows the results of modeling the RQFM-LFM signal with the following parameters: $f_0 = 0$, $\Delta f_1 = 550$ kHZ, $\Delta f_2 = 100$ kHz, $T_1 = 20$ μs, $T_2 = 40$ μs.

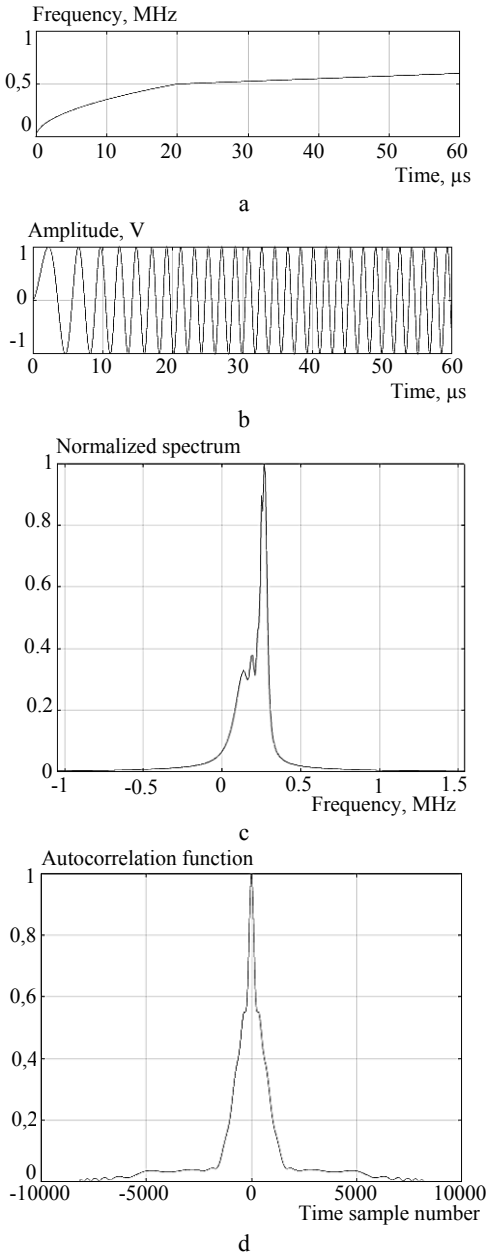

Figure 4 – Frequency change plot (a), oscillogram (b), spectrum (c), ACF (d) RQFM-LFM signal with parameters: $f_0 = 0$, $\Delta f_1 = 550$ kHz, $\Delta f_2 = 100$ kHz, $T_1 = 20$ μs, $T_2 = 40$ μs

The frequency change graph of Fig. 4a and the oscillogram of Fig. 4b indicate the absence of abrupt changes in the instantaneous frequency and phase of the signal, which also confirms the appearance of its spectrum of Fig. 4c. For better clarity of the result, the ACF plot is shown on a linear scale. The MPSLL value is –26.9 dB and the SLL decay rate is estimated at 30 dB/dec. ACF shows the merger of ML with SL, due to which its width at the minimum level has significantly expanded, however, at 0.707 from the maximum value that determines the discriminating ability from the range to the location objects, the ML ACF extension is acceptable.

The ratio of duration and frequency deviations of RQFM and LFM fragments is determined, according to which MMs ensure the absence of frequency and phase jumps (or only phase) at the junction of NLFM signal fragments. For the duration of fragments, the ratio of 1:2 is optimal, that is, the LFM fragment must be twice as long as the RQFM fragment. For frequency deviations, the range of change in the ratio between fragments is significantly larger – from 6:5 to 5:1. If this value is 1:1 and with a subsequent increase in the contribution of the LFM fragment to the ACF of the resulting signal, the RQFM increases and it begins to approach the ACF LFM signal in appearance and characteristics, which is quite logical.

6 DISCUSSION

The two-fragment NLFM signals considered in [35] mainly have the form LFM-LFM, the MPSLL obtained for this case is at the level of –16.5 dB, which is a very real result in the absence of phase jump compensation in MM shifted time, which was used. In [33], a two-fragment NLFM signal is proposed, the first fragment of which has an exponential FM, the smallest MPSLL ACF value is –25.96 dB at $B_S = 200$. As a result of the studies performed, this result was improved by 0.94 dB with $B_S = 39$, that is, such an MPSLL value is obtained for the low-base ($B_S < 100$) signal.

The achieved MRBP level of synthesized RQFM-LFM signals practically reaches (on average, about 1–2 dB worse) MPSLL three-fragment NLFM signals consisting of LFM fragments. However, compared to the latter, the new signals have a wider range of changes in the input frequency parameters and provide a higher SLL decay rate. Therefore, in the case of WP application, an improvement in the results of further MPSLL reduction as compared to the above signals is to be expected.

CONCLUSIONS

The scientific novelty. As a result of the studies, a new two-fragment NLFM signal was synthesized, which consists of RQFM and LFM fragments. Two new MMs (current time and with time shift) have been developed to calculate the instantaneous phase values of such a signal. Studies of MM have demonstrated their mutual compliance and adequacy, which is evidence of their reliability. The combination of RQFM and LFM fragments allows you to get an NLFM signal with a reduced MPSLL level and a higher SLL decay rate. A feature of using RQFM fragments in a two-fragment NLFM signal has been revealed. This feature is that to calculate the frequency parameters of the RQFM fragment, it is necessary to use the average value of FMR β_{1N}, and to determine the components of the frequency-phase correction, take the final

DOI 10.15588/1607-3274-2024-1-2

FMR value for the fragment, which is half the average, that is, $\beta_{1N}/2$. By mathematical modeling, it is determined that the MPSLL for the studied group of five NLFM signals ranges from –19.38 dB to –20.76 dB, and the SLL decay rate varies from 19 dB/dec to 22 dB/dec, which is on average more than in the case of using only LFM fragments. Comparison with the LFM-LFM type signal for the same frequency-time parameters demonstrates a decrease in MPSLL by 1.5 dB, an increase in the SLL decay rate by 6.5 dB/deck, however, the ML ACF width increased by 24%, which is the price for improving the previous characteristics. Analysis of the obtained oscillograms, spectra and ACF synthesized NLFM signals shows no distortion at the joints of fragments, which indicates that the values of frequency-phase (or only phase) jumps are determined correctly and fully compensated.

The practical significance of the obtained results lies in the possibility of using the synthesized NLFM signal for use as a probe in a variety of radar facilities. In addition to the above advantages RQFM-LFM signal is its insensitivity to change the ratio of frequency deviations RQFM and LFM fragments in contrast to LFM-LFM signals. That is, in the case of practical application, the RQFM-LFM type signal will provide greater variability in the frequency parameters of the probe signal without changing the total frequency deviation, which will improve the characteristics of the radar in terms of noise immunity and electronic compatibility.

Prospects for further research. In the future, it is planned to develop MM three-fragment NLFM signals that use fragments with a nonlinear law of frequency modulation.

ACKNOWLEDGEMENTS

We thank the management of Ivan Kozhedub Kharkiv National Air Force University for the opportunity to conduct scientific research.

REFERENCES

1. Lei T., Liang L. Research and design of digital unit for direct digital frequency synthesizer, International Conference on Electronic Materials and Information Engineering (EMIE 2021), *Journal of Physics: Conference Series,* 2021, Vol. 1907, №012004. DOI:10.1088/1742-6596/1907/1/012004.
2. Liu X., Luong H. C. A Fully Integrated 0.27-THz Injection-Locked Frequency Synthesizer With Frequency-Tracking Loop in 65-nm CMOS, *IEEE Journal of Solid-State Circuits,* 2020, Vol. 55, Issue 4, pp. 1051–1063. DOI: 10.1109/JSSC.2019.2954232.
3. Blackledge J. Digital Signal Processing. Dublin, Horwood Publishing, second edition, 2006, 840 p.
4. Li Tan. Digital Signal Processing. Fundamentals and Applications. Georgia, Academic Press, 2008, 816 p.
5. Zhang J., Zhang R., Dai Y. Design and FPGA implementation of DDS based on waveform compression and Taylor series, *2017 29th Chinese Control And Decision Conference (CCDC), 2017, Computer Science, Engineering,* pp. 1301–1306. DOI:10.1109/CCDC.2017.7978718.
6. Genovese M., Napoli E., De Caro D. et all. Analysis and comparison of Direct Digital Frequency Synthesizers implemented on FPGA, *Integration,* 2014, Vol. 47, Issue 2, pp. 261–271.
7. Anil A., Prasad A. FPGA Implementation of DDS for Arbitrary wave generation, International Journal of Engineering Research and Applications, 2021, Vol. 11, Issue 7, (Series-II) pp. 56–64. DOI: 10.9790/9622-1107025664.
8. Obadi A. B., Soh P. J., Aldayel O. et al. Detection Using Radar Techniques and Processing With FPGA Implementation, IEEE Circuits and Systems Magazine, 2021, Vol. 21, Issue 1, pp. 41–74.
9. Liao X., Zhang L., Hu X. et all. FPGA Implementation of a Higher SFDR Upper DDFS Based on Non-Uniform Piecewise Linear Approximation, Applied Sciences, 2023, Vol. 13, Issue 19, №10819. https://doi.org/10.3390/app131910819.
10. Vankka J. Digital Synthesizers and Transmitters for Software Radio. New York: Springer, 2005, 359 p. DOI. 10.1007/1-4020-3195-5.
11. Skolnik M. I. Radar Handbook. Editor in Chief. Boston, McGraw-Hill Professional, second edition, 1990, 846 p.
12. Cook C. E., Bernfeld M. Radar Signals: An Introduction to Theory and Application. Boston, Artech House, 1993, 552 p.
13. Levanon N., Mozeson E. Radar Signals. New York, John Wiley & Sons, 2004, 403 p.
14. Saleh M., Omar S.-M., E. Grivel et al. A Variable Chirp Rate Stepped Frequency Linear Frequency Modulation Waveform Designed to Approximate Wideband Non-Linear Radar Waveforms, Digital Signal Processing, 2021, Vol. 109, №102884.
15. Van Trees H. L. Detection, Estimation, and Modulation Theory. New York, John Wiley & Sons, 2004, 716 p.
16. Xu Z., Wang X., Wang Y. Nonlinear Frequency-Modulated Waveforms Modeling and Optimization for Radar Applications, *Mathematics,* 2022, Vol. 10, №3939. DOI: 10.3390/math10213939.
17. Meikle H. Modern radar systems. London, Artech House, second edition, 2008, 701 p.
18. Curry G. R. Radar System Performance Modeling. London, Artech House, second edition, 2004, 410 p.
19. Barton D. K. Radar System Analysis and Modeling. London, Artech House, 2005, 545 p.
20. Richards M. A., Scheer J. A., Holm W. A. Principles of modern radar. SciTech Publishing, 2010, 924 p.
21. Mervin C., Budge J., Shawn R. G. Basic Radar Analysis. London, Artech House, 2015, 727 p.
22. Melvin W. L., Scheer J. A. Principles of modern radar. New York, SciTech Publishing, 2013, 846 p.
23. Cook C.E. A class of nonlinear FM pulse compression signals, *Proc. IEEE,* 1964, Vol. 52, pp. 1369 – 1371.
24. Cook C. E, Paolillo J. A pulse compression predistortion function for efficient side lobe reduction in a high-power radar. Proceedings of the IEEE, 1964, Vol. 52(4), pp. 377–389. DOI: 10.1109/proc.1964.2927.
25. Heinzel G., Rüdiger A., Schilling R. Spectrum and spectral density estimation by the Discrete Fourier transform (DFT), including a comprehensive list of window functions and some new flattop windows [Electronic resource]. Access mode: https://pure.mpg.de/rest/items/item_52164_1/component/file_152163/content.
26. Doerry A. W. Catalog of Window Taper Functions for Side lobe Control [Electronic resource]. Access mode:

DOI 10.15588/1607-3274-2024-1-2

https://www.researchgate.net/publication/316281181_Catalog_of_Window_Taper_Functions_for_Sidelobe_Control.
27. Ghavamirad R., Sebt M. A. Side Lobe Level Reduction in ACF of NLFM Waveform, *IET Radar, Sonar & Navigation,* 2019, Vol. 13, Issue 1, pp. 74–80.
28. Chukka A., Krishna B. Peak Side Lobe Reduction analysis of NLFM and Improved NLFM Radar signal, *AIUB Journal of Science and Engineering (AJSE),* 2022, Vol. 21, Issue 2, pp. 125–131.
29. Parwana S., Kumar S. Analysis of LFM and NLFM Radar Waveforms and their Performance Analysis, *International Research Journal of Engineering and Technology (IRJET),* 2015, Vol. 02, Issue 02, pp. 334–339.
30. Zhao Y., Ritchie M., Lu X. et al. Non-continuous piecewise nonlinear frequency modulation pulse with variable subpulse duration in a MIMO SAR Radar System, Remote Sensing Letters, 2020, Vol. 11, Issue 3, pp. 283–292.
31. Jeyanthi J. E., Shenbagavalli A., Mani V.R.S. Study of Different Radar Waveform Generation Techniques for Automatic Air Target Recognition, *International Journal of Engineering Technology Science and Research (IJETSR),* 2017, Vol. 4, Issue 8, pp. 742–747.
32. Adithyavalli N. An Algorithm for Computing Side Lobe Values of a Designed NLFM function, International Journal of Advanced Trends in Computer Science and Engineering, 2019, Vol. 8, Issue 4, pp. 1026–1031. DOI:10.30534/ijatcse/2019/07842019.
33. Valli N. A., Rani D. E., Kavitha C. Modified Radar Signal Model using NLFM, *International Journal of Recent Technology and Engineering (IJRTE),* 2019, Vol. 8, Issue 2S3, pp. 513–516. DOI: 10.35940/ijrte.B1091.0782S319.
34. Kavitha C., Valli N. A., Dasari M. Optimization of two-stage NLFM signal using Heuristic approach, I*ndian Journal of Science and Technology,* 2020, Vol. 13(44), pp. 4465–4473. DOI:10.17485/IJST/v13i44.1841.
35. Chukka A., Krishna B. Peak Side Lobe Reduction analysis of NLFM and Improved NLFM Radar signal, *AIUB Journal of Science and Engineering (AJSE),* 2022, Vol. 21, Issue 2, pp. 125–131.
36. Fan Z., Meng H.-Y. Coded excitation with Nonlinear Frequency Modulation Carrier in Ultrasound Imaging System, *IEEE Far East NDT New Technology & Application Forum (FENDT)*. Kunming, Yunnan province, China, 20–22 November 2020, pp. 31–35.
37. Song C., Wang Y., Jin G. et al. A Novel Jamming Method against SAR Using Nonlinear Frequency Modulation Waveform with Very High Side Lobes, *Remote Sensing,* 2022, Vol. 14, Issue 21, №5370.
38. Xu W., Zhang L., Fang C. et al. Staring Spotlight SAR with Nonlinear Frequency Modulation Signal and Azimuth Non Uniform Sampling for Low Side Lobe Imaging, Sensors, 2021, Vol. 21, Issue 19, №6487. DOI: 10.3390/s21196487.
39. Swiercz E., Janczak D., Konopko K. Estimation and Classification of NLFM Signals Based on the Time-Chirp, *Sensors,* 2022, Vol. 22, Issue 21, № 8104. DOI: 10.3390/s22218104.
40. Kostyria O. O., Hryzo A. A., Dodukh O. M. et al. Mathematical model of a two-fragment signal with a non-linear frequency modulation in the current period of time, *Visnyk NTUU KPI Seriia – Radiotekhnika Radioaparatobuduvannia,* 2023, Vol. 92, pp. 60–67. DOI:10.20535/RADAP.2023.92.60-67.
41. Kostyria O. O., Hryzo A. A., Dodukh O. M. et al. Improvement of mathematical models with time-shift of two- and tri-fragment signals with non-linear frequency modulation, *Visnyk NTUU KPI Seriia – Radiotekhnika Radioaparatobuduvannia,* 2023, Vol. 93, pp. 22–30. DOI: 10.20535/RADAP.2023.93.22-30.

Received 08.01.2024.
Accepted 15.02.2024.

УДК 621.396.962

ДВОФРАГМЕНТНІ НЕЛІНІЙНО-ЧАСТОТНО МОДУЛЬОВАНІ СИГНАЛИ З КОРІНЬ-КВАДРАТИЧНИМ ТА ЛІНІЙНИМ ЗАКОНАМИ ЗМІНИ ЧАСТОТИ

Костиря О. О. – д-р техн. наук, с.н.с., пров. наук. співр. Харківського національного університету Повітряних Сил імені Івана Кожедуба, Харків, Україна.

Гризо А. А. – канд. техн. наук, доц., начальник НДЛ Харківського національного університету Повітряних Сил імені Івана Кожедуба, Харків, Україна.

Худов Г. В. – д-р техн. наук, проф., начальник кафедри Харківського національного університету Повітряних Сил імені Івана Кожедуба, Харків, Україна.

Додух О. М. – канд. техн. наук, пров. наук. співр. Харківського національного університету Повітряних Сил імені Івана Кожедуба, Харків, Україна.

Лісогорський Б. А. – канд. техн. наук, старш. наук. співр. Харківського національного університету Повітряних Сил імені Івана Кожедуба, Харків, Україна.

АНОТАЦІЯ

Актуальність. Бурхливий розвиток техніки цифрового синтезу та обробки радіолокаційних сигналів, який спостерігається у останні десятиліття, практично зняв обмеження щодо можливості реалізації довільних законів частотної модуляції радіоколивань. Поряд з традиційним застосуванням лінійно-частотно-модульованих сигналів в сучасних радіолокаційних засобах використовуються зондувальні сигнали з нелінійною частотною модуляцією, які забезпечують нижчий рівень максимальних бічних пелюсток та більшу швидкість їх спадання. Ці фактори в свою чергу сприяють покращенню характеристик виявлення цілей за умов дії пасивних завад, а також підвищенню ймовірності виявлення малорозмірних цілей на тлі цілей з більшими ефективними поверхнями розсіювання. У зв'язку з цим велика кількість досліджень проводиться у напрямку подальшого удосконалення існуючих та синтезу радіолокаційних сигналів з новими законами частотної модуляції. Використання багатофрагментних нелінійно-частотно-модульованих сигналів, до складу яких входять фрагменти як з лінійною, так і з нелінійною модуляцією забезпечує збільшення кількості можливих варіантів законів частотної модуляції та синтез сигналів з прогнозованими характеристиками. Синтез нових багатофрагментних сигналів зі зниженим рівнем бічних

DOI 10.15588/1607-3274-2024-1-2

пелюсток автокореляційних функцій та більшою швидкістю їх спадання є важливою науково-технічною задачею, вирішенню якої присвячено дану статтю.

Мета роботи – розробка математичних моделей поточного і зсунутого часу двофрагментних нелінійно-частотно модульованих сигналів для випадку, коли перший фрагмент має корінь-квадратичну, а другий лінійну частотну модуляцію та визначення доцільності використання такого сигналу в радіолокаційних застосуваннях.

Метод. В статті теоретично підтверджено, що для математичної моделі поточного часу, при переході від першого фрагменту до другого на стику фрагментів виникають стрибки миттєвої частоти та фази (або тільки фази для математичної моделі зсунутого часу), які можуть суттєво спотворити результуючий сигнал. Визначення величини частотно-фазових стрибків для їх подальшого усунення виконується шляхом знаходження різниці між значенням початкової фази другого фрагменту та кінцевим значенням фази першого. Відмінною особливістю розроблених математичних моделей є використання першого фрагменту сигналу з корінь-квадратичною, а другого – лінійною частотною модуляцією.

Результати. Порівняння сигналу, перший фрагмент якого має корінь-квадратичну частотну модуляцію, та сигналу з двома лінійно-частотно модульованими фрагментами за умови рівності сумарної тривалості та девіації частоти показує, що для нового синтезованого сигналу максимальний рівень бічних пелюсток знизився на 1,5 дБ, а швидкість їх спадання збільшилася на 6,5 дБ/дек.

Висновки. Синтезовано новий двофрагментний сигнал, перший фрагмент якого має корінь-квадратичну, а другий – лінійну частотну модуляцію. Розроблено математичні моделі поточного часу та зі зсувом часу для розрахунку значень миттєвої фази такого сигналу. Відмінною особливістю цих моделей є наявність складових для компенсації частотно-фазових спотворень з урахуванням закону модуляції частоти першого фрагменту. Отримані осцилограми, спектри та автокореляційні функції синтезованих двофрагментних сигналів не протирічать відомим теоретичним положенням, що свідчить про достовірність та адекватність запропонованих математичних моделей.

КЛЮЧОВІ СЛОВА: математична модель; нелінійна частотна модуляція; максимальний рівень бічних пелюсток.

ЛІТЕРАТУРА

1. Lei T. Research and design of digital unit for direct digital frequency synthesizer / T. Lei, L. Liang // International Conference on Electronic Materials and Information Engineering (EMIE 2021), Journal of Physics: Conference Series. – 2021, Vol. 1907. – №012004. DOI:10.1088/1742-6596/1907/1/012004.
2. Liu X. A Fully Integrated 0.27-THz Injection-Locked Frequency Synthesizer With Frequency-Tracking Loop in 65-nm CMOS / X. Liu, H. C. Luong // IEEE Journal of Solid-State Circuits. – 2020, Vol. 55, Issue 4. – P. 1051–1063. DOI: 10.1109/JSSC.2019.2954232.
3. Blackledge J. Digital Signal Processing / J. Blackledge – Dublin : Horwood Publishing, second edition, 2006. – 840 p.
4. Tan L. Digital Signal Processing. Fundamentals and Applications / L. Tan. – Georgia : Academic Press, 2008. – 816 p.
5. Zhang J. Design and FPGA implementation of DDS based on waveform compression and Taylor series / J. Zhang, R. Zhang, Y. Dai // 2017 29th Chinese Control And Decision Conference (CCDC), Computer Science, Engineering. – 2017. – P. 1301–1306. DOI:10.1109/CCDC.2017.7978718.
6. Analysis and comparison of Direct Digital Frequency Synthesizers implemented on FPGA / [M. Genovese, E. Napoli, D. De Caro et al.] // Integration. – 2014, Vol. 47, Issue 2. – P. 261–271.
7. Anil A. FPGA Implementation of DDS for Arbitrary wave generation / A. Anil, A. Prasad // International Journal of Engineering Research and Applications. – 2021, Vol. 11, Issue 7. – P. 56–64. DOI: 10.9790/9622-1107025664.
8. Detection Using Radar Techniques and Processing With FPGA Implementation / [A. B. Obadi, P. J. Soh, O. Aldayel et al.] // IEEE Circuits and Systems Magazine. – 2021, Vol. 21, №1. – P. 41–74.
9. FPGA Implementation of a Higher SFDR Upper DDFS Based on Non-Uniform Piecewise Linear Approximation / [X. Liao, L. Zhang, X. Hu et al.] // Applied Sciences. – 2023, Vol. 13, Issue 19. – №10819. https://doi.org/10.3390/app131910819.
10. Vankka J. Digital Synthesizers and Transmitters for Software Radio / J. Vankka – New York : Springer, 2005. – 359 p. DOI: 10.1007/1-4020-3195-5.
11. Skolnik M. I. Radar Handbook. Editor in Chief / M. I. Skolnik. – Boston : McGraw-Hill Professional, second edition, 1990. – 846 p.
12. Cook C. E. Radar Signals: An Introduction to Theory and Application / C. E. Cook, M. Bernfeld. – Boston : Artech House, 1993. – 552 p.
13. Levanon N. Radar Signals / N. Levanon, E. Mozeson. – Hoboken : John Wiley & Sons, 2004. – 403 p.
14. A Variable Chirp Rate Stepped Frequency Linear Frequency Modulation Waveform Designed to Approximate Wideband Non-Linear Radar Waveforms / [M. Saleh, S.-M. Omar, E. Grivel et al.] // Digital Signal Processing. – 2021. – Vol.109. – №102884.
15. Van Trees H. L. Detection, Estimation, and Modulation Theory / H. L. Van Trees. – Edition, reprint : John Wiley & Sons, 2004. – 716 p.
16. Xu Z. Nonlinear Frequency-Modulated Waveforms Modeling and Optimization for Radar Applications / Z. Xu, X. Wang, Y. Wang // Mathematics. – 2022. – Vol. 10, №3939.
17. Meikle H. Modern radar systems / H. Meikle. – London, Artech House, second edition, 2008. – 701 p.
18. Curry G. R. Radar System Performance Modeling / G. R. Curry. – London, Artech House, second edition, 2004. – 410 p.
19. Barton D. K. Radar System Analysis and Modeling / D. K. Barton. – London : Artech House, 2005. – 545 p.
20. Richards M. A. Principles of modern radar / M. A. Richards, J. A. Scheer, W. A Holm. – SciTech Publishing, 2010. – 924 p.
21. Mervin C. Basic Radar Analysis / C. Mervin, J. Budge, R. G. Shawn. – London, Artech House, 2015. – 727 p.
22. Melvin W. L. Principles of modern radar / W. L. Melvin, J. A. Scheer. – New York: SciTech Publishing, 2013. – 846 p.
23. Cook C. E. A pulse compression predistortion function for efficient side lobe reduction in a high-power radar / C. E. Cook, J. Paolillo // Proceedings of the IEEE. – 1964. – Vol. 52(4). – P. 377–389. DOI: 10.1109/proc.1964.2927.

DOI 10.15588/1607-3274-2024-1-2

24. Cook C.E. A class of nonlinear FM pulse compression signals / C. E. Cook // Proceedings of the IEEE. – 1964. – Vol. 52(11). – P. 1369–1371.
25. Heinzel G. Spectrum and spectral density estimation by the Discrete Fourier transform (DFT), including a comprehensive list of window functions and some new flattop windows [Electronic resource] / G. Heinzel, A. Rüdiger, R. Schilling. – Access mode: https://pure.mpg.de/rest/items/item_152164_1/component/file_152163/content.
26. Doerry A. W. Catalog of Window Taper Functions for Side lobe Control [Electronic resource] / A. W. Doerry. – Access mode: https://www.researchgate.net/publication/316281181_Catalog_of_Window_Taper_Functions_for_Sidelobe_Control.
27. Ghavamirad R. Side Lobe Level Reduction in ACF of NLFM Waveform / R. Ghavamirad, M. A. Sebt // IET Radar, Sonar & Navigation. – 2019. – Vol. 13, Issue 1. – P. 74–80.
28. Chukka A. Peak Side Lobe Reduction analysis of NLFM and Improved NLFM Radar signal / A. Chukka, B. Krishna // AIUB Journal of Science and Engineering (AJSE). – 2022. – Vol. 21, Issue 2. – P. 125–131.
29. Parwana S. Analysis of LFM and NLFM Radar Waveforms and their Performance Analysis / S. Parwana, S. Kumar // International Research Journal of Engineering and Technology (IRJET). – 2015. – Vol. 02, Issue 02. – P. 334–339.
30. Non-continuous piecewise nonlinear frequency modulation pulse with variable sub-pulseduration in a MIMO SAR Radar System / [Y. Zhao, M. Ritchie, X. Lu et al.] // Remote Sensing Letters. – 2020. – Vol. 11, Issue 3. – P. 283–292.
31. Jeyanthi J. E. Study of Different Radar Waveform Generation Techniques for AutomaticAir Target Recognition / J. E. Jeyanthi, A. Shenbagavalli, V.R.S. Mani // International Journal of Engineering Technology Science and Research (IJETSR). – 2017. – Vol. 4, Issue 8. – P 742–747.
32. Adithyavalli N. An Algorithm for Computing Side Lobe Values of a Designed NLFM function / N. Adithyavalli // International Journal of Advanced Trends in Computer Science and Engineering. – 2019. – Vol. 8, Issue 4. – P. 1026–1031. DOI:10.30534/ijatcse/2019/07842019.
33. Valli N. A. Modified Radar Signal Model using NLFM / N. A. Valli, D. E Rani, C. Kavitha // International Journal of Recent Technology and Engineering (IJRTE). – 2019. – Vol. 8, Issue 2S3. – P. 513–516. DOI: 10.35940/ijrte.B1091.0782S319.
34. Kavitha C. Optimization of two-stage NLFM signal using Heuristic approach / C. Kavitha, N. A. Valli, M. Dasari // Indian Journal of Science and Technology. – 2020. – Vol. 13(44). – P. 4465–4473. DOI:10.17485/IJST/v13i44.1841.
35. Chukka A. Peak Side Lobe Reduction analysis of NLFM and Improved NLFM Radar signal / A. Chukka, B. Krishna // AIUB Journal of Science and Engineering (AJSE). – 2022. – Vol. 21, Issue 2. – P. 125–131.
36. Fan Z. Coded excitation with Nonlinear Frequency Modulation Carrier in Ultrasound Imaging System / Z. Fan, H.-Y. Meng // IEEE Far East NDT New Technology & Application Forum (FENDT): Kunming, Yunnan province, China, – 20–22 Nov. 2020. – P. 31–35.
37. A Novel Jamming Method against SAR Using Nonlinear Frequency Modulation Wave-form with Very High Side Lobes / [C. Song, Y. Wang, G. Jin et al.] // Remote Sensing. – 2022. – Vol. 14, Issue 21. – №5370
38. Staring Spotlight SAR with Nonlinear Frequency Modulation Signal and Azimuth Non Uniform Sampling for Low Side Lobe Imaging / [W. Xu, L. Zhang, C. Fang et al.] // Sensors. – 2021. – Vol. 21, Issue 19. – №6487. DOI: 10.3390/s21196487.
39. Swiercz E. Estimation and Classification of NLFM Signals Based on the Time–Chirp / E. Swiercz, D. Janczak, K. Konopko // Sensors. – 2022. – Vol. 22, Issue 21. – № 8104. DOI: 10.3390/s22218104.
40. Mathematical model of a two-fragment signal with a nonlinear frequency modulation in the current period of time / [O. O. Kostyria, A. A. Hryzo, O. M. Dodukh et al.] // Visnyk NTUU KPI Seriia – Radiotekhnika Radioaparatobuduvannia. – 2023. – Vol. 92. – P. 60–67. DOI:10.20535/RADAP.2023.92.60-67.
41. Improvement of mathematical models with time-shift of two- and tri-fragment signals with non-linear frequency modulation / [O. O. Kostyria, A. A. Hryzo, O. M. Dodukh et al.] // Visnyk NTUU KPI Seriia – Radiotekhnika Radioaparatobuduvannia. – 2023. – Vol. 93. – P. 22–30. DOI: 10.20535/RADAP.2023.93.22-30.

DOI 10.15588/1607-3274-2024-1-2